Recovery of Chromium and Two Solvents (Dichloromethane-DCM Tetrachloroethane-TCE) Using Nanofiltration and Reverse Osmosis Membranes from Leather Industry Wastewater

DELİA TERESA SPONZA, RUKİYE ÖZTEKİN*
Department of Environmental Engineering
Dokuz Eylül University
Tınaztepe Campus, 35160 Buca/İzmir,
TURKEY
* Corresponding Author

Abstract: - In this study, for removal of the leather industry pollutants and to recovery of chromium (Cr), dichloromethane (DCM) and tetrachloroethane (TCE) two sequential nanofiltration (NF) (NF90 and NF270) and two reverse osmosis (RO) (BW30 and SW30) reactor membranes were used. The membrane surface properties were investigated by Fourier Transform Infrared Spectroscopy-Attenuated Total Reflectance (FTIR-ATR) and Scanning Electron Microscopy (SEM). The permeate of the SW30 reverse osmosis exhibited high removals varying between 98% and 99% for sodium ion (Na^+), potassium ion (K^+), magnesium ions (Mg^{2+}), calcium ions (Ca^{2+}), total chemical oxygen demand (COD_{total}), dissolved chemical oxygen demand (COD_{dis}), dissolved organic carbon (DOC) and inert chemical oxygen demand (inert COD), Chromium (Cr^{3+}), Dichloromethane and Tetrachloroethane. In the NF90 nanofiltration process lower removals were detected (96%-97%) for all pollutants mentioned above. The effluent of reverse osmosis with a BW30 membrane match to the Turkish Water Pollution Control Regulation rules for treated water discharged to the receiving environment while SW30 reverse osmosis membrane was perfect for ultimate treatment of the pollutants present in the leather industry discharges. From the concentrate of the SW30 reverse osmosis, 945 mg/l chromium, 460 mg/l dichloromethane and 360 mg/l tetrachloroethane were reused. The performance and recoveries of Cr and two solvents (DCM and TCE) data in NF and RO membrane reactors were evaluated with Artificial Neural Network (ANN) process and Kruskal Wallis test statistic coupled with Mann-Whitney U statistic in this study.

Key-Words: - Artificial neural network (ANN); Chromium; Dichloromethane (DCM); Mann-Whitney U statistic; Leather industry wastewater; Nanofiltration (NF) membranes; Reverse osmosis (RO) membranes; Tetrachloroethane (TCE); Total dissolved solid (TDS); Transmembrane pressure (TMP).

Received: June 9, 2023. Revised: March 13, 2024. Accepted: April 17, 2024. Published: May 16, 2024.

1 Introduction

Wastewaters contained a lot of pollutants due to activities of the industry and extent globalization, [1]. The emissions coming from industrial discharges increased linearly, [2]. The leather/tanning industry contained a lot of pollutants affecting the ecosystems negatively, [3], [4]. In the tanning process a lot of chemicals was used, [4], [5]. Among them, the chromium (Cr) salts like chromium (III) sulphate affect negatively the aquatic environments if the leather wastewater was not treated effectively, [6], [7], [8], [9]. A big part of Cr is used during processing the animal skins. The rest of the Cr is emitted to the whole treatment plant. Therefore, the effluents of the leather industry wastewaters exhibited toxic effects to the soils, reservoirs and aquatic ecosystems, [10], [11].

Tannery, is the main production process of the leather industry; and in this process the hides and skins of animals are used to make various leather products, [12]. The discharge of this industry wastewater into the receiving environment as a result of utilization of higher volume of water during the production phase is an important problem in terms of environmental pollution. Furthermore, the tannery industry makes a significant contribution to the country's export earnings, [13]. Approximately 31.4 million kg of skin are processed annually in Turkey, [14]. From 3000 liter of tannery discharges 100 kg of hides were produced, [15]. In chromium tanning process, 276 chemicals and 14 heavy metals are used. This caused to a big water pollution, [16]. Since the leather industry process consume large volumes of water the wastes contained huge quantities of liquids.

The effluent qualities are far from the desired level for acceptance due to heavy load of pollutants like Cr, chlorides (Cl), sodium (Na), dissolved solids (DS), Biological oxygen demand (BOD), COD, nitrogen (N_2) and total suspended solids (TSS) and solvents namely Dichloromethane and Tetrachloroethane, [17]. Cr has more importance in leather industry since the amounts of released Cr(VI) with time, owing to the simultaneous release of reducing agents from the leather. Significantly more Cr(III) than Cr(VI) was released from the Cr-tanned leather for all conditions tested; Cr was used for complexation of some carboxylate in leather processing, [18]. Tanning involves fixing solvents onto the leather surface. This creates a problem sometimes for efficiency of reaction, because there is typically competition between the leather and the solvent. When the reagent is partitioned between the two environments, dependent on the relative affinities of the reactivities. The reduced affinity of the solvent for the leather, typically basic Cr(III) salts, makes the substrates more attractive to the reagent and hence reaction is accelerated.

Problem of Cr disposal can be greatly minimized if recovery of the Cr is possible. Numerous physical and chemical methods such as adsorption, [19], sedimentation, [20], electrochemical processes, [21], [22], biological operations, [5], cementation, [23], coagulation/flocculation, [24], filtration and membrane processes, [25], [26], chemical precipitation and solvent extraction, [27], [28], have been employed for the minimization of the pollution level in wastewater. However, with this processes reuse of chemical merit compounds like chromium, DCM and TCE was not possible. Few methods like membrane separation technology are used for the treatment and for the recovery of some merit chemicals, [29]. Membrane separation is a process in which a semi permeable membrane is used to retain species of low molecular weight and a pressure is applied as driving force to revert the solvent natural tendency of passing from a more diluted solution to another more concentrated one, [30].

The dominance of pressure-driven membrane processes in wastewater treatment, such as reverse osmosis (RO) and nanofiltration (NF), were extensively used in industrial applications for reuse of the pollutants, [31]. This is mainly due to the fact that these processes are mature and, consequently, by usage of suitable membranes the solvents can be easily recovered, [32]. In addition, recent studies have shown that NF and RO, were the most promising technologies for providing high-quality wastewater treatment and recoveries of chemical merits organic and inorganic substances, [33], [34].

The semi-permeable membrane is a thin film that is constructed by different materials and it is assembled in order to support a high Trans-membrane pressure. There are four types of industrial developed membrane separation processes which are microfiltration (MF), ultrafiltration (UF), RO and electrodialysis (ED), [35]. The range of application of these pressure-driven membrane is dependent to the water separation processes via molecular sieving through increasingly fine pores, [36]. Although, RO, and UF are conceptually similar processes, the difference depends to their pore diameters by the differences in the membranes used, [37]. With this impression an attempted has been made for eco-friendly recovery and recycling technologies for the treatment of wastewater before their disposal.

Utilization of the suitable wastewater treatment plants was very important and some operational conditions affect the efficiency of the treatment processes. The physicochemical treatment processes like coagulation and flocculation, and bacterial processes can be used, however excess sludge production limited the usage of these treatment processes, [7].

In last decade, membrane treatment processes are extensively used since their costs were low and they were used in the treatment of leather industry wastewater, [7], [38], [39], [40], [41], [42]. The permeate of the membranes was effectively treated and reuse of chromium, DCM and TCE solvents provides high economical advantageous. Studies applying RO, [7], and UF, [38], have been reported. Sometimes, some problems with the pores of the membranes like fouling can be occurred. By utilizations of correct operational conditions, the aforementioned problem can be solved. In the membrane separation processes Cr ions are also successfully remediated. For example, by using a RO and a sequential RO/NF process 90% and 95%, [43], [44], [45], pollutant yields were detected.

Membrane technology, especially NF is considered a viable option for water treatment because of its efficiency for Cr removal. It can operate at low pressures and can provide a good permeation flow rate, [46], [47], [48]. It can also recover, entirely or partially, most of the salts present (mono-, di- and trivalent forms) and has the potential to concentrate them.

RO treatment processes provide the recovery of the permeate of a leather industry. This cause to reduce the cost spent for water consumption, [7], while UF and MF membrane processes permeates contains some bigger pollutants since the pore size on their membranes were bigger in the comparison to

RO membranes before emitted to the receiving places, [42], [43].

The aim of this study was the removal of the leather industry pollutants and recoveries of Cr, DCM and TCE solvents in two NF (NF270 and NF90) and two RO (BW30 and SW30) membranes. The membrane surface properties were determined by FTIR-ATR and SEM. Na^+, K^+, Mg^{2+} and Ca^{2+}, COD_{total}, COD_{dis}, DOC and inert COD maximum removal yields were investigated. Furthermore, the optimum operational conditions for maximum yields of pollutants in the leather industry permeate were investigated.

2 Materials and Methods

2.1 Characterization of Raw Leather Industry wastewater

The characterization of the pollutants present in a raw leather industry wastewater was tabulated in Table 1. The results of the analysis were repeated 3 times under laboratory conditions and the average values were mentioned (Table 1).

* Table 1 can be found in the Appendix section.

2.2 NF and RO Membranes

Two NF (NF270, NF90) and two RO (BW30, SW30) membrane processes were used in this study (Midland, MI, USA). The properties of the membranes used were summarized in Table 2. The membranes used in this study exhibited hydrophilic properties and the measured water contact angles ($\theta < 90°$) were 29° for NF270, 51° for NF90, 55° for BW30 and 62° for SW30, [49]. NF270 membrane exhibited low sodium chloride (NaCl) rejections (Table 2), while NF90 and BW30 were a tight NF and a loose RO membrane, respectively, [50]. SW30 is extensively utilized for treat the saline wasters, [30].

* Table 2 can be found in the Appendix section.

2.3 Experimental Set up and Parameters

The experiments were performed under laboratory conditions. The area of the membrane was 56 cm^2 and the reactor consisted from stainless-steel with an disc. The pressure was adjusted from 10 to 40 atm for NF and RO membranes, respectively. Before all experimental studies, pre-precipitation process and granulated activated carbon (GAC) filtration were applied to the raw leather industry wastewater. Then, sequential NF/RO membrane system experiments were performed.

In this study, all experiments were carried out at a constant temperature (30°C). The effect of increasing transmembrane pressures (TMP) (3, 6 and 12 atm) on fluxes (10, 25 and 40 l/m^2h) and on the removals of pollutant parameters were examined in NF at 30°C. Similarly, the effects of increasing TMP pressures (10, 25 and 40 atm) to flowrate (5, 10 and 20 l/m^2h), and to removals of pollutants were investigated at 30°C in RO at 30°C.

2.4 Solvent Extraction and Purification Process

The purification of DCM and TCE solvents were performed by extraction procedure according to Standard Methods 6232-B by Liquid-liquid extraction gas chromatographic methods, [51].

2.5 Characterizations of Membrane Surface Properties

2.5.1 FTIR-ATR Spectral Measurements

FTIR measurements were carried out using a FTIR spectrometer (Thermo Scientific- 50) equipped with a germanium (Ge) ATR device (Thermo Scientific, Smart ARKTM). The effective dimensions of the Ge crystal are 47 mm × 5 mm. The refractive index of the Ge is 4 and the angle of incidence in our device was 45°, generating 12 reflections. The calculated depth of penetration is 0.664 μm and the calculated effective pathlength is 2.59 μm. The radiation from the infrared (IR) source of the spectrometer was focused into the attenuated total reflection (ATR) crystal and the output radiation (from the other side of the crystal) was focused onto a cooled MCT (mercury cadmium telluride) detector. Measurements were carried out in the spectral range of 650–4000 cm^{-1}. Each spectrum was an average of 64 scans to increase the signal to noise ratio (SNR).

2.5.2 SEM Analysis

The morphological features and structure of the membrane samples were determined by a JSM-840A electron microscope (JEOL, Tokyo, Japan). The samples were cleaned with ethanol to obtain clear images. The samples were dried with a low-speed vacuum system. Degreasing and drying of the samples were performed to reduce outgassing caused by organic impurities and wastewater in the sample. SEM images were obtained with a JSM-840A electron microscope (JEOL, Tokyo, Japan).

2.6 Analytical Procedure

pH, T(°C), TSS, Total volatile suspended solids (TVSS), Biological oxygen demand 5-days (BOD_5), COD_{total}, COD_{dis}, inert COD, DOC, Total organic carbon (TOC) and fecal coliform bacteria were monitored according to Standard Methods 2550, 2580, 2540 D, 2540 E, 5210 B, 5220 D, 5220 E, 5220C, 9217A, 5520, 9225 respectively, [51]. Ammonium nitrogen (NH^{4+}-N], nitrate nitrogen (NO^{3-}-N), chloride ion (Cl^-), boron (III) ions [B(III)], Na^+, sodium carbonate ($NaCO_3$), sulfate ion (SO_4^{2-}), total phosphorus (Total-P) and total nitrogen (Total-N) were measured with cell test spectroquant kits (Merck, Germany) at a spectroquant NOVA 60 (Merck, Germany) spectrophotometer (2003).

Total chrome [chromium (III) ions Cr(III) and chromium (VI) ions Cr(VI) sum] analysis was performed according to SM3500 in Inductively Coupled Plasma-Mass Spectrometer (ICP-MS) device. [43], Spectral interferences occur mainly due to polyatomic and isobaric ions, which have the same mass-to-charge ratios (m/z^+) as the analyte of interest. The determination of chromium was performed by ICP-MS, four Cr isotopes (^{50}Cr, ^{52}Cr, ^{53}Cr, and ^{54}Cr) with natural abundances varied between 2.4% and 83.8%.

The measurement of color was carried out following the approaches described by Olthof and Eckenfelder, [52], and Eckenfelder, [53]. According to these methods, the color content was determined by measuring the absorbance at three wavelengths (445 nm, 540 nm and 660 nm), and taking the sum of the absorbances at these wavelengths. Sodium adsorption ratio (SAR) means a value representing the relative amount of sodium ions (Na^+) to the combined amount of calcium (Ca^{2+}) and magnesium (Mg^{2+}) ions in water using the following formula in Eq. (1):

$$SAR = \frac{[Na^+]}{\sqrt{\frac{[Mg^{2+}]+[Ca^{2+}]}{2}}} \quad (1)$$

where all concentrations are expressed as milliequivalents of charge per liter (mEq/l).

2.7 Regulation of Water Pollution Control for Treated Wastewater

The water pollution control Regulation classify the treated irrigation waters. This technical procedure was published in the Turkey in the official newspaper at January 7, 1991, with a number of 20748, [54]. Referring to the limits of given by this Regulation the leather industry effluents can be reused and can be used as 2. Class and 1. Class water with "good" and "very good" properties (Turkey Water Pollution Control Regulation, Date of update: RG-17122022-32046, from Table 12 (Table 3), [55].

* Table 3 can be found in the Appendix section.

2.8 Artificial Intelligence (AI) Models

In the wastewater treatment process, artificial intelligence (AI) models could be employed to minimize complexities, [56]. AI model is applicable to predicting the performance of water treatment, designing the key components, optimizing the operating parameters, evaluating the effluent quality, designing the treatment units, optimizing the pollutants, by predicting maintenance strategies using fault diagnosis, optimizing the energy efficiency of treatment processes, operating instructions based on performance, and making the systems fully automated. During the past few decades, by the usage of AI-based models in wastewater treatments an increase in treatment yields was detected. To achieve the best outcomes, these methods must be chosen considering the treatment system mechanism and the aim for which they are employed, [57].

Applications of AI models in wastewater treatment are the treatment plant performance, modelling of wastewater, optimization of water treatment, control on water treatment and predictive energy optimization, respectively.

In recent years, several soft computing tools and approaches have been applied to the prediction of water quality and associated variables, [58], [59], [60], [61], [62], [63], [64], and artificial neural networks (ANNs), [58], [65], [66], [67], [68]. ANN process involves the computations of input and output data.

2.8.1. Artificial Neural Network (ANN) Model

The ANNs always consist of three layers including (i) input, (ii) hidden, and (iii) output layers. The outputs of a neuron are calculated using Eq. (2):

$$o = f\left(\sum_{j=0}^{n} \omega_j \, x \, X_j\right) \quad (2)$$

where, n: is the input number, x_j: is the jth input to the neutron, ω_j: is the jth synaptic weight, and f: is a non-linear function, respectively.

For converting output data between – 1 and + 1, the hyperbolic tangent formula was applied as Eq. (3):

$$\tanh(x) = \frac{2}{1+e^{-2x}} - 1 \quad (3)$$

During the training process of input and output data set, the network weights are adjusted to achieve the similar outputs as seen in the training data set. For this purpose, the data were divided into two subsets for training model and validation purposes.

The Pearson correlation coefficient (r^2) and mean standard error (MSE) were computed to evaluate the performance of the developed models according to Eq. (4) and Eq. (5), [69]:

$$r^2 = 1 - \frac{\sum_{i=1}^{N}(y_{pre,i} - y_{exp,i})^2}{\sum_{i=1}^{N}(y_{pre,i} - y_{ave})^2} \quad (4)$$

$$MSE = \frac{1}{N}\sum_{i=1}^{N}(|y_{pre,i} - y_{exp,i}|)^2 \quad (5)$$

2.9 Other Statistical Analysis

Differences of removal efficiencies depending on TMP and fluxes determined by performing a non-parametric Kruskal–Wallis test followed by a Mann–Whitney U-test, [70]. The Mann–Whitney U-test was used to evaluate the relationship between pollutant yields and TMP. All results are reported at a significance level of $p \leq 0.01$, [71]. Multiple regression analysis between y and x variables was performed using the SPSSWIN in Microsoft Windows™, [72]. The linear correlation was assessed with r^2. r^2 is the correlation coefficient and reflects statistical significance between dependent and independent variables.

3 Results and Discussions

3.1 Characterizations of NF and RO Membranes

3.1.1 FTIR-ATR Analysis

The FTIR-ATR spectrum of NF (NF270, NF90) and RO (BW30, SW30) membranes used to treat and reuse 3 components in leather industry wastewater was shown in Fig. 1. The main peaks of FTIR-ATR spectrum for NF270 (red spectrum) were observed at 1600 cm^{-1}, 1480 cm^{-1}, 1280 cm^{-1}, 1175 cm^{-1}, 1150 cm^{-1} and 860 cm^{-1} at wavenumbers, respectively (Fig. 1a). The main peaks of FTIR-ATR spectrum for NF90 (blue spectrum) were obtained at 1500 cm^{-1}, 1440 cm^{-1}, 1280 cm^{-1}, 1175 cm^{-1} and 860 cm^{-1} wavenumbers, respectively (Fig. 1a). The main peaks of FTIR-ATR spectrum for BW30 (red spectrum) were determined at 3250 cm^{-1}, 1650 cm^{-1}, 1500 cm^{-1}, 1250 cm^{-1}, 1150 cm^{-1}, 1000 cm^{-1} and 550 cm^{-1} wavenumbers, respectively (Fig. 1b). The main peaks of FTIR-ATR spectrum for SW30 (blue spectrum) were measured at 1400 cm^{-1}, 1350 cm^{-1}, 1250 cm^{-1}, 750 cm^{-1}, 600 cm^{-1} and 550 cm^{-1} wavenumbers, respectively (Fig. 1b).

* Fig. 1 can be found in the Appendix section.

NF270 and NF90 are made of semi-aromatic polyamide obtained by interfacial polymerization between trimesoyl chloride (TMC) and piperazine. The active layers of BW30, SW30 membranes are made of a full aromatic polyamide obtained by interfacial polymerization between TMC and m-phenylenediamine (MPD). ATR-FTIR spectra of BW30 and SW30 membranes indicated that four spectra are similar for wave numbers between 860 and ~1600 cm^{-1}. Due to the relatively deep penetration depth of the signal both the polysulfone sublayer and the polyamide skin layer were probed. The bands at 1541 and 1580 cm^{-1} are assignable to the fully aromatic polyamide skin layers of the membrane. As mentioned above, the spectra are identical for wave numbers lower than 1600 cm^{-1}, which confirms that the same chemical functions are present in the membranes. For both BW30 and SW30 membranes, the overlap of the N-H stretching band of amide groups and that of the O-H stretching band of carboxylic acid functions resulting from the incomplete cross-linking of the polyamide skin layer leads to an additional shoulder peak at 1450 cm^{-1}. The shoulder peak corresponding to N-H stretching vibration is absent in the spectra of both BW30 and SW30 membranes. Both BW30 and SW30 membranes are coated with additional surface coating materials results in stronger stretching vibrations of aliphatic C-H between 1300 and 1390 cm^{-1}. However, in our study, there was no significant difference among the four membranes in the range of 1220 ~ 1390 cm^{-1}.

3.1.2 SEM Analysis

The morphological features of NF (NF270, NF90) and RO (BW30, SW30) membranes were characterized through SEM images (Fig. 2). The SEM images of NF270 (Fig. 2a), NF90 (Fig. 2b), BW30 (Fig. 2c) and SW30 (Fig. 2d) membranes treating the leather industry wastewater was separately illustrated (SEM images scale was 200 nm).

* Fig. 2 can be found in the Appendix section.

As can be seen, the SEM images for NF90 and RO (BW30 and SW30) were virgin and used membranes were similar, indicating that neither fouling occurred nor were elements stacked in the membrane surface during the high-concentrated filtration tests. However, the membrane surface images for NF270 before and after use indicated changes during its performances. As mentioned previously, linearity of permeate flux and TMP indicates that membrane fouling and compaction effects are negligible.

3.2 Effect of TMP on NF Flux and Total Dissolved Solid (TDS) Rejection in NF

The effect of increasing TMP (3, 6 and 12 atm) on the flux variations on NF (NF270 and NF90) were examined at 30°C treating the leather industry wastewater (Fig. 3). As the TMP was increased from 3 atm to 6 and to 8 atm, the flux in the NF270 increased from 10.20 l/ m^2.h to 21.20 and 39 l/m^2.h while the fluxes elevated to 15 l/ m^2.h, 28 and 37.90 l/m^2.h in the NF90 at at 30°C (Fig. 3).

* Fig. 3 can be found in the Appendix section.

It was found that the flux increase is higher in RO reactor than that NF. The permeate flux is highly depends on the numbers of the pores in the membrane surface and inside membrane which the wastewater is going to pass the membrane and to the extent of adsorption process. Furthermore, the type of interactions taking place between the emulsion droplets and the membrane material such as hydrophobic/hydrophilic interactions and hydrogen (H_2) bonding by Van der Waals interactions and electrostatic effects affect the permeate flux.

78%, 71% and 60% TDS rejection yields were obtained at 3, 6 and 12 atm TMP, respectively, on NF270 membrane process at 30°C (Fig. 4). 82%, 74% and 66% TDS rejection yields were found at 3, 6 and 12 atm TMP, respectively, on NF90 at 30°C (Fig. 4). It was found that as the TMP was increased, the TDS rejections decreased.

* Fig. 4 can be found in the Appendix section.

This difference in rejection at different transmembrane pressures can be explained as follows: When a new membrane was introduced to treat the wastewater during the low transmembrane pressure experiments, rapid pore blockage was not occurred in this study. This would have tightened the membrane and caused increased rejection of smaller contaminants over time. At high transmembrane pressures the rejection percentages of TDS decreased since ions and other dissolved pollutant parameters inhibits the passage of treated water from the pores and a big problem of fouling of membrane pores was occurred in NF reactor.

The fluxes in NF reactor containing NF270 and NF90 membranes exhibited similar responses to the TMPs (Mann–Whitney U-test statistic = 1.23, p = 0.05). The Kruskal–Wallis U test statistics showed that effect of TMP on flux is significant since the Kruskal–Wallis test statistics are not differed (Mann–Whitney U-test statistic = 1.14, p = 0.05). Similarly, a linear relationship between TDS rejection yields and TMP was detected and this is significant ((Mann–Whitney U-test statistic = 1,32, p = 0.05).

The Kruskal–Wallis test statistics showed that the TAAs removals are differed after 150 min sonication versus increasing temperature and these differences are significant (Mann–Whitney U-test statistic = 13.88, p = 0.05).

3.3 Effect of TMP on RO Flux and TDS Rejection in RO

The TMP was increased from 3 atm, to 6 and to 12 atm in the RO at 30°C to detect the TMP impact on fluxes treating the leather industry wastewater (Fig. 5). As the TMP was increased, the flux also elevated from 25 l/m^2.h, to 38 and to 60 l/m^2.h in BW30 while the fluxes increased from 7 l/m^2.h, to 41 and to 65 l/m^2.h in SW30 RO reactor versus increasing of pressures from 3 atm to 6 and to 12 atm at 30°C (Fig. 5).

* Fig. 5 can be found in the Appendix section.

As the TMP was increased the permeation fluxes also were increased. In this study, 12 atm TMP did not affect the polymeric structure of membrane. Furthermore, 12 atm TMP did not cause to a cake layer formation on the membrane surface to compress the SW30 membrane in RO. This accelerates the membrane fouling, [73].

87%, 79% and 70% TDS rejection yields were obtained at 3, 6 and 12 atm TMP, respectively, in RO reactor containing BW30 membrane at 30°C (Fig. 6). 90%, 82% and 75% TDS rejection yields were observed at 3, 6 and 12 atm TMP, respectively, on SW30 at 30°C (Fig. 6). As the TMP increased, the TDS rejection percentages decreased in RO.

* Fig. 6 can be found in the Appendix section.

The fluxes in RO reactor containing BW30 and SW30 membranes exhibited similar responses to the TMPs (Mann–Whitney U-test statistic = 1.19, p = 0.05). The Kruskal–Wallis U test statistics showed that effect of TMP on flux is significant since the Kruskal–Wallis test statistics are not differed (Mann–Whitney U-test statistic = 1.14, p = 0.05). Similarly, a linear relationship between TDS rejection yields and TMP was detected in RO and this is significant (Mann–Whitney U-test statistic = 1,20, p = 0.05).

With increase in pressure across the membrane, the flux increases and the relation between the flux and pressure is exactly linear indicating the existence of an additional resistance besides the membrane resistance (Fig. 6). An increase in TMP results in decreasing of TDS rejection without approaching to a limiting value.

The TDS rejections is high in the RO reactor compared to the NF membrane reactor. The feedwater passes through the membrane, the ions and organics are left behind and the permeate rejection remains between 60% to 82% for TDS. Permeate recoveries for TDS are typically limited to 82% in RO because of the limited solubility of the dissolved left behind in the reject. TDS rejection is a function of transmembrane pressure and the highest TDS rejection was detected in RO reactor containing SW30 membrane as expected. NF membranes, provided the lowest TDS rejections.

3.4 The Removal Efficiencies of Some Pollutants in the Leather Industry Wastewater after NF and RO Treatment

High pollutant yields were detected in RO reactor with SW-30 membrane compared to NF 270 and NF90 membrane reactors. Maximum 99% COD_{total}, 98% COD_{dis}, 98% DOC, 98% Inert COD, 99% Na^+, 99% K^+, 99% Mg^{2+}, 99% Ca^{2+} removals were detected after treatment with BW30 RO membrane process at 30°C and at a pH of 3.6. The SW30 RO reactor effluent exhibited high removal varying between 98% and 99% for Na^+, K^+, Mg^{2+} and Ca^{2+}, COD_{total}, COD_{dis}, DOC and inert COD compared to NF90 membrane process (Table 4).

* Table 4 can be found in the Appendix section.

This observation indicates that the RO membrane has high rejection for all pollutants and a significant rejection for all pollutants were detected. The Kruskal–Wallis U test statistics exhibited a significant linear regression between pollutant yields and fluxes in RO (Mann–Whitney U-test statistic = 1,18, p = 0.05). The Kruskal–Wallis U test statistics showed a linear regression between pollutant yields and fluxes in NF (Mann–Whitney U-test statistic = 1.18, p = 0.05). This relationship is not significant since the Kruskal–Wallis test statistics are differed (Mann– Whitney U-test statistic = 12.22, p = 0.07).

The effluents of the RO reactor with SW-30 and BW30 membranes match to the limits given by The Turkish Regulation in Table 3 for re- utilization of treated wastewater as irrigation purpose based on TSS, SO_4^{-3}. NH_3, Cr, fecal coliform, NO_3-N, NH_3, TOC concentrations (data not shown). The effluents of NF reactor with 90 and 270 membranes were not suitable for utilization.

The studies performed in this study were correlated with some recent studies treating the leather industry: In a study performed by the performances of two NF (200 and 400 molecular weight cut offs) and two RO (1000 molecular weight cut offs) membranes, [74]. In this study lower TDS rejections and removal efficiencies for TSS, SO_4^{3-}. NH_3, Cr, fecal coliform, NO_3-N, NH_3, TOC, COD and COD dis were detected in RO reactor. The removal of leather industry wastewater by NF and RO reactors with membranes having pore diameters of 150–300 Da and < 100 Da was investigated, [75]. Similar recoveries and pollutants yields were detected. The lower recoveries for Cr and DCM solvent (89% and 88%, respectively) were found in a RO with a membrane of SW30, [76], [77].

3.5 Recoveries of Cr, DCM and TCE in Leather Industry Wastewater with NF and RO Membranes

Leather tanning procedure mainly depends on chrome tanning. A huge amount of basic chromium sulphate [BCS, $Cr(OH)SO_4$] is used in leather tanning. About 60% – 70% of BCS has been taken by leather and the rest of the amount is discharged as effluent and solid waste. The effluent which contained a high concentration of Cr is precipitated as solid chromium hydroxide [$Cr(OH)_3$] with other elements which is called a chrome cake. On the other hand, chromium (III) sulfate [$Cr_2(SO_4)_3$] has been considered as the most effective and efficient tanning agent formed by some poly-chromium compounds with a process called olation acts as active compounds in tanning which crosslinking with collagen subunits. Cr with its +6-oxidation state is referred as Cr(VI). There is a high risk of getting cancers to the workers exposed to Cr(VI) for a prolonged time. One of the cleaner processing options recommended is that the Cr which is let out in the effluent, may be recovered for reuse to ensure not only economy of usage of Cr, but also effective management of this toxic substance.

Chrome recovery plants can be established to meet different scales of production starting from individual small-scale tannery to a group of tanneries. for common chrome recovery.

In this study solvent and chromium recoveries were performed from the retentates of NF and RO membrane reactors. Cr, DCM and TCE recoveries from tanning exhausted baths represents a significant economic advantage for leather industry in terms of its reuse and for the simplification of the polishing process. In this study from the retentate/concentrate of the RO containing SW30 membrane 99% Cr, DCM and TCE recoveries were detected. 945 mg/l Cr, 460 mg/l DCM and 360 mg/l TCE was detected from the retentate of the leather industry wastewater (Table 5).

* Table 5 can be found in the Appendix section.

Cr, DCM and TCE recovery percentages varied between 77% and 82% in NF reactor. Recovery percentages of RO reactor containing BW30 membrane exhibited 95%, 91% and 88% maximum recoveries for Cr, DCM and TCE, respectively. The recovered concentrations from the retentate of this RO reactor were 870 mg/l Cr, 400 mg/l DCM and 300 mg/l TCE.

It was found that the recoveries of the aforementioned chemicals having economical merits is higher in RO reactor containing SW 30 membrane. In other words, the best potential in terms of providing adequate effluent permeate quality and offering the possibility for Cr, DCM and TCE recoveries was obtained by using a RO reactor containing SW30 membrane at pH=3.6 and at a temperature of 30ºC.

3.6 Comparison of Experimental Yields with ANN Procedure, Pearson Correlation Coefficient (r^2) and Mean Standard Error (MSE)

A comparison between the removal efficiencies of pollutants and recoveries in leather industry wastewater after NF and RO treatment processes were performed with ANN model by taken into consideration the Pearson correlation coefficient (r^2) and the mean standard error (MSE) data (Table 6). These results were given for SW30 membrane in RO reactor for 30ºC temperature (Table 6).

* Table 6 can be found in the Appendix section.

The ANN model worked as an excellent AI model in this study due to its lowest mean standard errors and highest Pearson correlation coefficient (r^2) values. The observed results indicated that the simulation model based on the ANN is practical and revealed that this model was successful. According to in the results given in Table 6 all the mean standard errors were very small both in RO and NF membrane reactors. Pearson correlation coefficient (r^2) for the yields and recoveries in RO reactors were 0.99 indicating the linear correlation between pollutant and yields where the yields were high (99%). However, the Pearson correlation coefficient in effluent and recoveries are slightly lower (0.96-0.98) in NF membrane reactor.

In another study, ANN statistical analysis showed that there is a linear regression between COD removal, time, pH, concentration, and the molar ratio of hydrogen, [78], [79]. The performance of a wastewater treatment facility was evaluated using AI-model, [80]. They found that pH, temperature, dissolved oxygen, BOD, and COD affect significantly performance of an NF reactor, [80]. They achieved acceptable correlation coefficients with maximum contaminant removal efficiency of 87.68%, [80]. An ANN-based linear regression model was used to determine water quality parameters. The findings revealed that the ANN statistical analysis program evaluated the performance of wastewater, as the results were also confirmed by error analyses and regression coefficient values, [80].

3.7 Recommendations for Operational Maintenance of Membrane Reactors

Cleaning in place (CIP) is a procedure for cleaning the interior of the RO system's membranes. Membrane CIP allows cleaning without dismantling the wastewater treatment system. In the CIP process; sing a cleaning solution, the membrane is cleaned and rinsed. Thus, the removal of contaminants accumulated on the membrane surface during standard operations is ensured.

Feedwater and system design will affect the operation of the membrane in a RO system. The type of chemicals to be used for CIP depends on the type of pollutant. For example, a high pH cleaning solution can be used to clean biological material. A low pH cleaner should be preferred to remove mineral deposits.

Both cleaning chemicals are needed in most environments. Low pH cleaning before high pH cleaning should generally be the most effective method. However, each treatment plant has different characteristics. Cleaning is like an art; It can be developed by trial and error according to the characteristics of the treatment plant. To identify specific contaminants on the membrane surface and how best to remove them; Autopsy of the membrane may be considered.

The utilization of formulated CIP chemicals extends the operating time of the system, reduce the cleaning frequency and increase the productive life of the RO system elements.

High flow and low pressure are the most effective methods of removing contaminants from the membrane system. The final rinse ensures that all cleaning chemicals are removed from the membrane. Quality rinsing aims to ensure that product quality is restored within acceptable operating conditions.

3.8 Cost Evaluations for Sequential NF/RO Membrane System

Energy use and carbon footprint of water consumption emerge as critical issues in the development of membrane reactors for clean water production. Therefore, the correlation between water and energy consumption, also known as water-energy coupling effect. This is very important for the development of a sustainable and low-cost membrane treatment system. The growth of water resources should not bring about high-cost energy consumption. Due to their high energy and separation efficiency, membrane-based technologies have gained widespread application in various wastewater treatment processes.

Solar-powered RO plants allow eliminating fossil fuel dependence for the production of sufficient purified industrial water.

It is of great importance to verify the possible applicability of zero liquid discharge (ZLD) process in membrane treatment. ZLD process is a water treatment approach in which all wastewater is treated and recycled, resulting in zero discharge at the end of the treatment cycle. ZLD process relates the residual output in terms of waste, wastewater and energy loss to the process input based on materials and energy. ZLD process; Allowing the possibility of using a process cycle in which wastewater treatment is envisaged for the recycling of water, taking into accounts the mass balance and energy balance of materials other than water.

The use of solar energy can reduce some of the high operating cost of the membrane process, but the high capital investment for a solar PV system poses a significant financial challenge for most developing countries.

4 Conclusions

The permeate of the SW30 RO membrane reactor exhibited high removals varying between 98% and 99% for Na^+, K^+, Mg^{2+} and Ca^{2+}, COD_{total}, COD_{dis}, DOC and inert COD compared to NF90 membrane. As the TMP was increased the fluxes were also increased in both reactors. As the TMP was increased the TDS rejections were decreased in both reactors. The RO permeate containing SW30 membrane match with rules given by Turkish Water and Wastewater Regulations and can be emitted to the receiving media. From the retentate/concentrate of the SW30 membrane 945 mg/l Cr, 460 mg/l DCM and 360 mg/l TCE were reused.

The ANN model worked as an excellent AI model in this study due to its lowest error and highest coefficient values. The observed results indicated that the simulation model based on the ANN is practical.

The NF membrane can be used as a pre-treatment for the RO membrane to produce high quality water and reduce contaminant concentrations, thereby minimizing the potential for fouling.

It is of great importance to verify the possible applicability of ZLD process in wastewater treatment. ZLD process is a water treatment approach in which all wastewater is treated and recycled, resulting in zero discharge at the end of the treatment cycle.

In our further studies, it is planned to operate a sequential NF/RO membrane process to ensure maximum efficiencies for pollutants and recover of the chemical merit compounds from the leather industry wastewater.

Acknowledgement:
Experimental analyzes in this study were performed at the Laboratories of the Canada Research Center, Ottawa, Canada. The authors would like to thank this body for providing financial support.

References:

[1] E. Raper, T. Stephenson, D.R. Anderson, R. Fisher, A. Soares, Industrial wastewater treatment through bioaugmentation, *Process Safety and Environmental Protection,* Vol.118, 2018, pp. 178–187.
[2] A. Wondie, W. Assefa, Bahir Dar tannery effluent characterization and its impact on the head of Blue Nile River, *African Journal of Environmental Science and Technology,* Vol.8, No.6, 2014, pp. 312–318.
[3] M. Chowdhury, M.G. Mostafa, T.K. Biswas, A. Mandal, A.K. Saha, Characterization of the effluents from leather processing industries, *Environmental Processes,* Vol.2, 2015, pp. 173–187.
[4] M., Jin, F. Lian, R. Xia, Z. Wang, Formulation and durability of a geopolymer based on metakaolin/tannery sludge, *Journal of Waste Management,* Vol.79, 2018, pp. 717–728.
[5] D.M. Angelucci, V. Stazi, J. Andrew, A.J. Daugulis, M.C. Tomei, Treatment of synthetic tannery wastewater in a continuous two-phase partitioning bioreactor: biodegradation of the organic fraction and chromium separation,

Journal of Cleaner Production, Vol.152, 2017, pp. 321–329.

[6] E. Kiliç, J. Font, R. Puig, S. Çolak, D. Çelik, Chromium recovery from tannery sludge with saponin and oxidative remediation, *Journal of Hazardous Materials,* Vol.185, 2011, pp. 456–462.

[7] G. Lofrano, S. Meriç, G.E. Zengin, D. Orhon, Chemical and biological treatment technologies for leather tannery chemicals and wastewaters: a review, *Science of the Total Environment,* Vol.461–462, 2013, pp. 265–281.

[8] P. Kavouras, E. Pantazopoulou, S. Varitis, G. Vourlias, K. Chrissafis, G.P. Dimitrakopulos, M. Mitrakas, A.I. Zouboulis, T. Karakostas, A. Xenidis, Incineration of tannery sludge under oxic and anoxic conditions: study of chromium speciation, *Journal of Hazardous Materials,* Vol.283, 2015, pp. 672–679.

[9] D.A.L. Vignati, B.J.D. Ferrari, J.-L. Roulier, M. Coquery, E. Szalinska, A. Bobrowski, A. Czaplicka, A. Kownacki, J. Dominik, Chromium bioavailability in aquatic systems impacted by tannery wastewaters, Part 1: Understanding chromium accumulation by indigenous chironomids, *Science of the Total Environment,* Vol.653, 2019, pp. 401–408.

[10] G. Vidal, J. Nieto, K. Cooman, M. Gajardo, C. Bornhardt, Unhairing effluents treated by an activated sludge system, *Journal of Hazardous Materials,* Vol.112, No.1-2, 2004, pp. 143–149.

[11] C. Agustini, M. Costa, M. Gutterres, Biogas production from tannery solid wastes—scale-up and cost saving analysis, *Journal of Cleaner Production*, Vol.187, 2018, pp. 158–164.

[12] P. Kumari, S. Malik, J. Bora, S. Mondal, R. Rani, A. Kapoor, *Chapter 18 - Applied aspects of reverse osmosis technology for industrial wastewater treatment*, in book: Development in Wastewater Treatment Research and Processes (Advanced Oxidation Processes for Tannery Effluent), 2024, pp. 341-366.

[13] Z. Abebe, Tannery Wastewater Management Problems in Ethiopia the Case of Batu Tannery, Addis Ababa University, College of Development Studies, Center for Environment, Water and Development, Department of Environment and Development, Bishoftu, Ethiopia, Master Thesis, May, 2011.

[14] A. Behailu, Assessment of Pre- and Post-Slaughter Hide and Skin Defects and Their Association with Carcass Condemnation in two Woredas of East Arsi Zone, Ethiopia, Addis Ababa University, College of Veterinary Medicine and Agriculture, Department of Tropical Animal Production and Health, Bishoftu, Ethiopia, Master Thesis, June 2015.

[15] H. Strathmann, L. Giorno, E. Drioli, Introduction to Membrane Science and Technology, 544, Wiley-VCH, Weinheim, Germany, 2011.

[16] K. Ramasamy, R. Naidu, Status of tanning industries in India, towards better management of soils contaminated with tannery waste, Workshop on Agriculture University, Coimbatore, India, 1998.

[17] M. Bosnic, J. Buljan, R.P. Daniels, Pollutants in tannery effluents, United Nations Industrial Development Organization, US/RAS/92/120, United States, 2000.

[18] H. Li, Z. Li, T. Liu Xiao, Z. Peng, L. Deng, A novel technology for biosorption and recovery hexavalent chromium in wastewater by bio-functional magnetic beads, *Bioresource Technology,* Vol.99, No. 14, 2008, pp. 6271–6279.

[19] T.T. Ha, V.A. Quan, N. Q. Hop, T.M. Thuy, N.T. Ngoc, L.X. Que, Studying on the adsorption of chromium (VI) on polyaniline modified with activated tea residue, *Vietnam Journal of Chemistry,* Vol.56, No.5, 2018, pp. 559–563.

[20] R. Michalski, M. Jabło´nska-Czapla, S. Szopa, A. Lyko, K. Grygoyc, Variability in different antimony, arsenic and chromium species in waters and bottom sediments of three water reservoirs in Upper Silesia (Poland): a comparative study, *International Journal of Environmental Analytical Chemistry,* Vol.96, No.7, 2016, pp. 682–693.

[21] A. Deghles, U. Kurt, Treatment of tannery wastewater by a hybrid electrocoagulation/electrodialysis process, *Chemical Engineering and Processing - Process Intensification,* Vol.104, 2016, pp. 43–50.

[22] W. Jin, H. Du, S. Zheng, Y. Zhang, Electrochemical processes for the environmental remediation of toxic Cr(VI): a review, *Electrochimica Acta,* Vol.191, 2016, pp. 1044–1055.

[23] C.R. Johnson, N.D. Shindgikar, M.M. Beurel, Overcoming environmental and technical challenges for well cementing: a global perspective, *SPE Production and Operations,* Vol.32, No.01, 2017, pp. 12–27.

[24] B. Mella, A.C. Glanert, M. Gutterres, Removal of chromium from tanning wastewater and its reuse, *Process Safety and Environmental Protection,* Vol.95, 2015, pp. 195–201.

[25] Y. Bao, X. Yan, W. Du, X. Xie, Z. Pan, J. Zhou, L. Li, Application of amine-functionalized MCM-41 modified ultrafiltration membrane to remove chromium (VI) and copper (II), *Chemical Engineering Journal,* Vol.281, 2015, pp. 460–467.
[26] S. Koushkbaghi, A. Zakialamdari, M. Pishnamazi, H. F. Ramandi, M. Aliabadi, M. Irani, Aminated-Fe_3O_4 nanoparticles filled chitosan/PVA/PES dual layers nanofibrous membrane for the removal of Cr(VI) and Pb(II) ions from aqueous solutions in adsorption and membrane processes, *Chemical Engineering Journal*, Vol.337, 2018, pp. 169–182.
[27] A.A. Nayl, H. F. Aly, Solvent extraction of V(V) and Cr(III) from acidic leach liquors of ilmenite using Aliquat 336, *Transactions of Nonferrous Metals Society of China,* Vol.25, No.12, 2015, pp. 4183–4191.
[28] C.R. Borra, B. Blanpain, Y. Pontikes, K. Binnemans, T. Van Gerven, Recovery of rare earths and major metals from bauxite residue (red mud) by alkali roasting, smelting, and leaching, *Journal of Sustainable Metallurgy,* Vol.3, No.2, 2017, pp. 393–404.
[29] C.H. Neoh, Z.Z. Noor, N.S.A. Mutamim, C.K. Lim, Green technology in wastewater treatment technologies: integration of membrane bioreactor with various wastewater treatment systems, *Chemical Engineering Journal, V*ol.283, 2016, pp. 582–594.
[30] R.W. Baker, Membrane Technology and Applications, (2nd ed.). John Wiley & Sons: Chichester, West Sussex, United Kingdom, pp. 206–207, 2004.
[31] N., Kabay, N.M.A. Shirazi, E. Güler, M. Bryjak, Grand challenges in membrane modules and processes, *Frontiers in Membrane Science and Technology*, Vol.1, No.4, 2022, pp. 1-4, 913597.
[32] M.D. Guiver, Field grand challenge for membrane science and technology, *Frontiers in Membrane Science and Technology*, Vol.1, No.2, 2022, pp. 1-7, 878879.
[33] T.A. Siddique, N.K. Dutta, N.R. Choudhury, Nanomaterials nanofiltration for arsenic removal: challenges, recent developments, and perspectives, *Nanomaterials*, Vol.10, No.7, 2020, 1323.
[34] C.N. Worou, Z.-L. Chen, T. Bacharou, Arsenic removal from water by nanofiltration membrane: Potentials and limitations, *Water Practice and Technology*, Vol.16, No.2, 2021, pp. 291–319.
[35] T. Subramani, D. Haribalaji, Biodegradation of tannery effluent and designing the reactor for clarifier and activated sludge process, *International Journal of Engineering Research,* Vol.2, No.3, 2012, pp. 774–781.
[36] G. Crawford, E. Fleischer, J. Lozier, G. Daigger, The evolution of membrane bioreactor system designs for wastewater treatment, *International Water Irrigation,* Vol.21, No.4, 2001, pp. 42–44.
[37] K. Parameshwaran, C. Visvanathan, Recent developments in membrane technology for wastewater reuse, In: Proceedings of the 6th International Conference on Advanced Wastewater Treatment, 14. Recycling and Reuse. Milan, Italy, pp. 16–19, 1998.
[38] J.A. Mendoza-Roca, M.V. Galiana-Aleixandre, J. Lora-García, A. Bes-Piá, Purification of tannery effluents by ultrafiltration in view of permeate reuse, *Separation and Purification Technology, V*ol.70, No.3, 2010, pp. 296–301.
[39] P. Religa, A. Kowalik, P. Gierycz, A new approach to chromium concentration from salt mixture solution using nanofiltration, *Separation and Purification Technology,* Vol.82, 2011, pp. 114–120.
[40] J. Dasgupta, D. Mondal, S. Chakraborty, J. Sikder, S. Curcio, H. A. Arafat, Nanofiltration based water reclamation from tannery effluent following coagulation pretreatment, *Ecotoxicology and Environmental Safety,* Vol.121, 2015, pp. 22–30.
[41] V. Colla, T.A. Branca, F. Rosito, C. Lucca, B. P. Vivas, V. M. Delmiro, Sustainable reverse osmosis application for wastewater treatment in the steel industry, *Journal of Cleaner Production*, Vol.130, 2016, pp. 103–115.
[42] I. G. Wenten, Khoiruddin, Reverse osmosis applications: prospect and challenges, *Desalination,* Vol.391, 2016, pp. 112–125.
[43] A. Karunakaran, A. Chaturvedi, J. Ali, R. Singh, S. Agarwal, M.C. Garg, Response surface methodology-based modeling and optimization of chromium removal using spiral-wound reverse-osmosis membrane setup, *International Journal of Environmental Science and Technology*, Vol.19, 2022, pp. 5999–6010.
[44] I. Fuoco, A. Figoli, A. Criscuoli, G. Brozzo, R. De Rosa, B. Gabriele, C. Apollaro, Geochemical modeling of chromium release in natural waters and treatment by RO/NF membrane processes, *Chemosphere*, Vol.254, 2020, 126696.
[45] S. Fadhil, Sustainable chromium removal by nanofiltration membranes: Application of pore flow model, *International Journal of Environmental Science and Technology*, Vol.20, No.4, 2023, pp. 8391–8398.

[46] I.M. Noël, R. Lebrun, C.R. Bouchard, Electro-nanofiltration of a textile direct dye solution, *Desalination,* Vol.129, No.2, 2000, pp. 125-136.
[47] Y. Xu, R.E. Lebrun, Comparison of nanofiltration properties of two membranes using electrolyte and non-electrolyte solutes, *Desalination,* Vol.122, No.1, 1999, pp. 95-105.
[48] J. Tanninen, M. Nyström, Separation of ions in acidic conditions using NF, *Desalination,* Vol.147, No.1-3, 2002, pp. 295-299.
[49] K.L. Tu, L.D. Nghiem, A.R. Chivas, Coupling effects of feed solution pH and ionic strength on the rejection of boron by NF/RO membranes, *Chemical Engineering Journal,* Vol.168, 2011, pp. 700–706.
[50] H.T. Madsen, E.G. Søgaard, Applicability and modelling of nanofiltration and reverse osmosis for remediation of groundwater polluted with pesticides and pesticide transformation products, *Separation and Purification Technology,* Vol.125, 2014, pp. 111–119.
[51] W.C. Lipps, E.B. Braun-Howland, T.E. Baxter, Standard Methods for the Examination of Water and Wastewater, (24th edition). W.C. Lipps, E.B. Braun-Howland, T.E. Baxter, (editors), American Public Health Association (APHA), American Water Works Association (AWWA), Water Environment Federation (WEF), Elevate Your Standards. American Public Health Association 800 I Street, NW Washington DC: 20001-3770, United States of America, December 1, 2022.
[52] M. Olthof, W.W. Eckenfelder, Coagulation of Textile Wastewater, Research Triangle Park, N.C., American Association of Textile Chemists and Colorists, Textile chemists and colorist, 8, 1976, pp. 18-22, ISSN: 0040-490X, Bib ID: 2287867.
[53] W.W. Eckenfelder, Industrial Water Pollution Control, (2nd ed.), Singapore: McGraw-Hill Inc, 1989.
[54] Turkey Water Pollution Control Ordinance in the water pollution control ordinance, the classification of irrigation waters, technical procedures communique of January 7, was published in 1991, 20748 in the Turkey Official Newspaper, Turkey, 1991.
[55] Turkey Water Pollution Control Regulation (Date of Update: RG-17122022-32046) Table 12: The wastewater of leather, leather products and similar industries is discharged to the receiving environment, Turkey, 17.12.2022.
[56] Y. Pan, F. Froese, N. Liu, Y. Hu, M. Ye, The adoption of artificial intelligence in employee recruitment: The influence of contextual factors, *International Journal of Human Resource Management*, Vol.33, No.7, 2021, pp. 1125–1147.
[57] A. Malviya, D. Jaspal, Artificial intelligence as an upcoming technology in wastewater treatment: A comprehensive review, *Environmental Technology Reviews*, Vol.10, No.1, 2021, pp. 177–187.
[58] V. Nourani, G. Elkiran, S. Abba, Wastewater treatment plant performance analysis using artificial intelligence—An ensemble approach, *Water Science and Technology*, Vol.78, No.10, 2018, pp. 2064–2076.
[59] Y. Kim, S. Oh, Machine-learning insights into nitrate-reducing communities in a full-scale municipal wastewater treatment plant, *Journal of Environmental Management*, Vol.300, 2021, 113795.
[60] F. Hernández-del-Olmo, E. Gaudioso, N. Duro, R. Dormido, Machine learning weather soft-sensor for advanced control of wastewater treatment plants, *Sensors*, Vol.19, No.14, 2019, 3139.
[61] S. Heo, K. Nam, S. Tariq, J.Y. Lim, J. Park, C. Yoo, A hybrid machine learning–based multi-objective supervisory control strategy of a full-scale wastewater treatment for cost-effective and sustainable operation under varying influent conditions, *Journal of Cleaner Production*, Vol.291, 2021, 125853.
[62] A. Bernardelli, S. Marsili-Libelli, A. Manzini, S. Stancari, G. Tardini, D. Montanari, G. Anceschi, P. Gelli, S. Venier, Real-time model predictive control of a wastewater treatment plant based on machine learning, *Water Science and Technology*, Vol.81, No.11, 2020, pp. 2391–2400.
[63] G. Elkiran, V. Nourani, S. Abba, Multi-step ahead modelling of river water quality parameters using ensemble artificial intelligence-based approach, *Journal of Hydrology*, Vol.577, No.2-4, 2019, 123962.
[64] P. Yu, J. Cao, V. Jegatheesan, X. Du, A real-time BOD estimation method in wastewater treatment process based on an optimized extreme learning machine, *Applied Sciences*, Vol.9, No.3, 2019, 523.
[65] S. Khademikia, A. Haghizadeh, H. Godini, G. Shams Khorramabadi, The performance evaluation of Khorramabad wastewater treatment plant by using artificial intelligence network, *Yafte,* Vol.18, No.3, 2016, pp. 12–23.
[66] J.-J. Zhu, L. Kang, P.R. Anderson, Predicting influent biochemical oxygen demand: Balancing

energy demand and risk management, *Water Research*, Vol.128, 2018, pp. 304–313.

[67] H. Kang, S. Yang, J. Huang, J. Oh, Time series prediction of wastewater flow rate by bidirectional LSTM deep learning, *International Journal of Control, Automation and Systems*, Vol.18, 2020, pp. 3023–3030.

[68] V. Mateo Pérez, J.M. Mesa Fernández, J. Villanueva Balsera, C. Alonso Álvarez, A random forest model for the prediction of FOG content in inlet wastewater from urban wwtps. *Water*, Vol.13, No.9, 2021, 1237.

[69] U. Özdemir, B. Özbay, S. Veli, S. Zor, Modeling adsorption of sodium dodecyl benzene sulfonate (SDBS) onto polyaniline (PANI) by using multi linear regression and artificial neural networks, *Chemical Engineering Journal*, Vol.178, 2011, pp. 183-190.

[70] S. Safarian, R. Unnthorsson, C. Richter, Performance analysis and environmental assessment of small-scale waste biomass gasification integrated chp in Iceland, *Fermentation*, Vol.197, 2020, 117268.

[71] S. Safarian, S.M.E. Saryazdi, R. Unnthorsson, C. Richter, Artificial neural network integrated with thermodynamic equilibrium modeling of downdraft biomass gasification-power production plant, *Energy*, Vol.213, 2020, 118800.

[72] S. Safarian, R. Unnthorsson, C. Richter, Techno-economic and environmental assessment of power supply chain by using waste biomass gasification in Iceland, *Biophysical Economics and Sustainability*, Vol.5, No.7, 2020, pp. 1-13.

[73] T. Mohammadi, M. Kazemimoghadam, M. Saadabadi, Modeling of membrane fouling and flux decline in reverse osmosis during separation of oil in water emulsion, *Desalination,* Vol.157, 2003, pp. 369-375.

[74] M.K. Purkait, V. Dinesh Kumar, D. Maity, Treatment of leather plant effluent using NF followed by RO and permeate flux prediction using artificial neural network, *Chemical Engineering Journal*, Vol.151, No.1-3, 2009, pp. 275-285.

[75] F. Yang, X.-B. Wang, Y. Shan, C. Wu, R. Zhou, N. Hengl, F. Pignon, Y. Jin, Research recap of membrane technology for tannery wastewater treatment: a review, *Collagen and Leather*, Vol.5, (2023), 1-17, Article number: 24.

[76] N.N.R. Ahmad, W.L. Ang, Y.H. Teow, A.W. Mohammad, N. Hilal, Nanofiltration membrane processes for water recycling, reuse and product recovery within various industries: A review, *Journal of Water Process Engineering*, Vol.45, 2022, 102478.

[77] A. Zaman, A. Ghosh, S. Santra, J. Chakraborty, J.T. Orasugh, D. Chattopadhyay, *Polymeric Nanocomposite Membranes for Treatment of Industrial Effluents*, In Book: Membranes for Water Treatment and Remediation, 2023, pp. 55–89.

[78] E.S. Elmolla, M. Chaudhuri, M.M. Eltoukhy, The use of artificial neural network (ANN) for modeling of COD removal from antibiotic aqueous solution by the Fenton process, *Journal of Hazardous Materials*, Vol.179, No.1-3, 2010, pp. 127–134.

[79] A. Bernardelli, S. Marsili-Libelli, A. Manzini, S. Stancari, G. Tardini, D. Montanari, G. Anceschi, P. Gelli, S. Venier, Real-time model predictive control of a wastewater treatment plant based on machine learning, *Water Science and Technology*, Vol.81, No.11, 2020, pp. 2391–2400.

[80] Zakmout, A.; Sadi, F.; Portugal, C.A.M.; Crespo, J.G.; Velizarov, S. Tannery effluent treatment by nanofiltration, reverse osmosis and chitosan modified membranes, *Membranes*, Vol.10, No.12, 2020, 378.

Contribution of Individual Authors to the Creation of a Scientific Article (Ghostwriting Policy)

Prof. Dr. Delia Teresa Sponza and Post-Dr. Rukiye Öztekin took an active role in every stage of the preparation of this article.

The authors equally contributed in the present research, at all stages from the formulation of the problem to the final findings and solution.

Sources of Funding for Research Presented in a Scientific Article or Scientific Article Itself

This research study was undertaken in the Environmental Microbiology Laboratories at Dokuz Eylül University Engineering Faculty Environmental Engineering Department, İzmir, Turkey. The authors would like to thank this body for providing financial support.

Conflict of Interest

The authors have no conflicts of interest to declare that are relevant to the content of this article.

APPENDIX

Table 1. Characterization of raw leather industry wastewater.

Parameters	Units	Concentrations
Total chemical oxygen demand (COD_{total})	mg/l	12967
Dissolved chemical oxygen demand (COD_{dis})	mg/l	2576
Inert chemical oxygen demand (inert COD)	mg/l	387
Dissolved organic carbon (DOC)	mg/l	1000
Total nitrogen (Total–N)	mg/l	14
Total phosphorus (Total–P)	mg/l	44
Color	A	8.23
pH		5.5
Total chrome [Cr (III) and Cr (VI) sum]	mg/l	569
Total organic carbon (TOC)	mg/l	1800
Sulfate (SO_4)	mg/l	1200
Percentage of Exchangeable Sodium (% Na)	% Na	50
Sodium adsorption rate (SAR)	mEq/l	22
Sodium carbonate residue (RSC)	mg/l	134
Chloride (Cl^-)	mg/l	338
Sulfate ion (SO_4^{2-})	mg/l	456
Total salt concentration	mg/l	963
Boron ion [B(III)]	mg/l	1.56
Nitrate nitrogen (NO_3^- - N)	mg/l	20
Ammonium nitrogen (NH_4^+-N)	mg/l	20
Fecal coliform bacteria	1/100 ml	60
Biological oxygen demand 5-days (BOD_5)	mg/l	75
Total suspended solids (TSS)	mg/l	45
Total volatile suspended solids (TVSS)	mg/l	27
Temperature [T(ºC)]	ºC	35
Acute toxicity 25% inhibition values ($EC_{25}x10^{-6}$)	mg/l	1380
Dichloromethane (DCM);	mg/l	220
Tetrachloroethane (TCE)	mg/l	180

Table 2. Characteristics of the NF and RO membranes

Membranes	Average Water Contact Angles (θ)	Maximum T(°C)	Maximum Pressure (atm)	Salt Rejection
NF270	29°	45	25	70% (NaCl), 60% ($CaCl_2$), 98.99% ($MgSO_4$)
NF90	51°	35-45	41	90%-96% (NaCl)
BW30	55°	45	41	99.40% (NaCl), 99.40% ($CaCl_2$), 99.70% ($MgSO_4$)
SW30	62°	45	69	99.40% (NaCl)

Table 3. Irrigation water quality parameters based on the classification of irrigation waters

Quality criteria	Irrigation water class				
	1. Class Water (Very Good)	**2. Class Water (Good)**	**3. Class Water (Usable)**	**4. Class Water (Must be used with Caution)**	**5.Class Water (Harmful) Not Available**
$EC_{25}x10^{-6}$	0-250	250-750	750-2000	2000-3000	> 3000
Percentage of Exchangeable Sodium (% Na)	< 20	20-40	40-60	60-80	> 80
Sodium adsorption rate (SAR) (mEq/l)	< 10	10-18	18-26	> 26	
Sodium carbonate residue (RSC) (mg/l)	< 66	66-133	> 133		
Chloride (Cl^-), (mg/l)	0-142	142-249	249-426	426-710	> 710
Sulfate (SO_4^{2-}) (mg/l)	0-192	192-336	336-575	575-960	> 960
Total salt concentration (mg/l)	0-175	175-525	525-1400	1400-2100	> 2100
Boron [B(III)] (mg/l)	0-0.5	0.5-1.12	1.12-2.0	> 2.0	-
Irrigation water class	C_1S_1	C_1S_2, C_2S_2, C_2S_1	C_1S_3, C_2S_3, C_3S_3, C_3S_2, C_3S_1	C_1S_4, C_2S_4, C_3S_4, C_4S_4, C_4S_3, C_4S_2, C_4S_1	-
NO_3^- (mg/l)	0-5	5-10	10-30	30-50	> 50
NH_4^+ (mg/l)	0-5	5-10	10-30	30-50	> 50
Fecal coliform - 1/100 ml	0-2	2-20	20-100	100-1000	> 1000
BOD_5 (mg/l)	0-25	25-50	50-100	100-200	> 200
Suspended solid (SS) (mg/l)	20	30	45	60	> 100
pH	6.5-8.5	6.5-8.5	6.5-8.5	6.5-9	9
Temperature	30	30	35	40	> 40

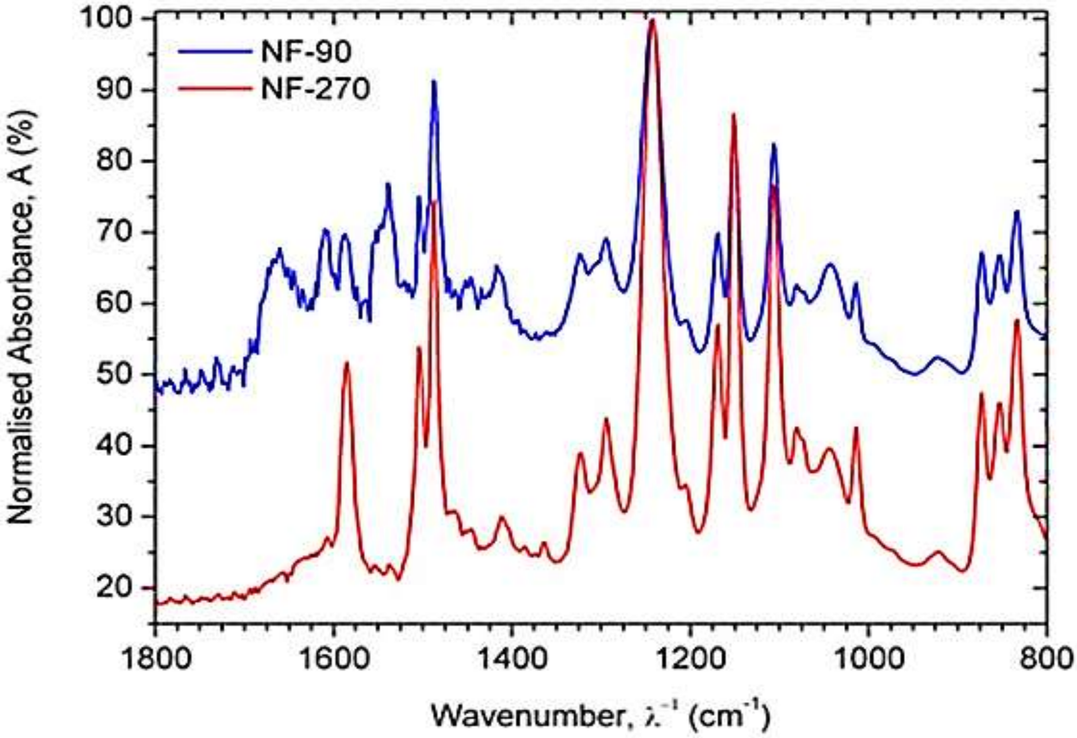

(a)

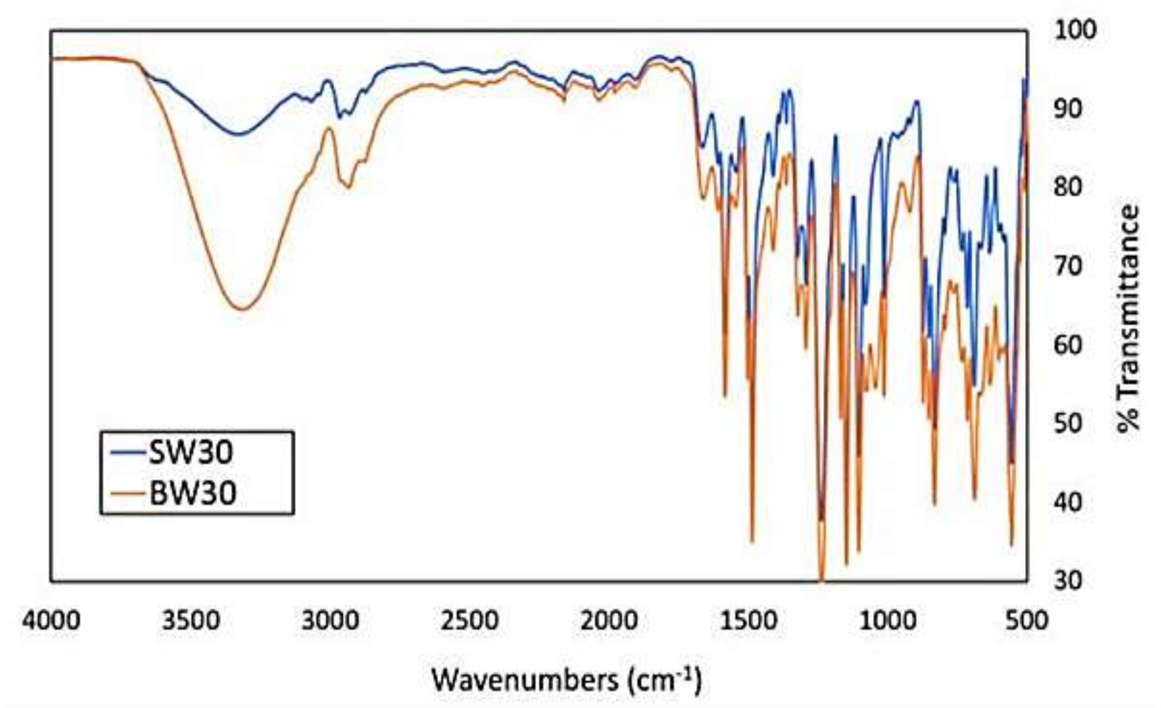

(b)

Fig. 1. FTIR-ATR spectrum of **(a)** NF270 (red spectrum), NF90 (blue spectrum) and **(b)** BW30 (red spectrum), SW30 (blue spectrum) membranes in leather industry wastewater.

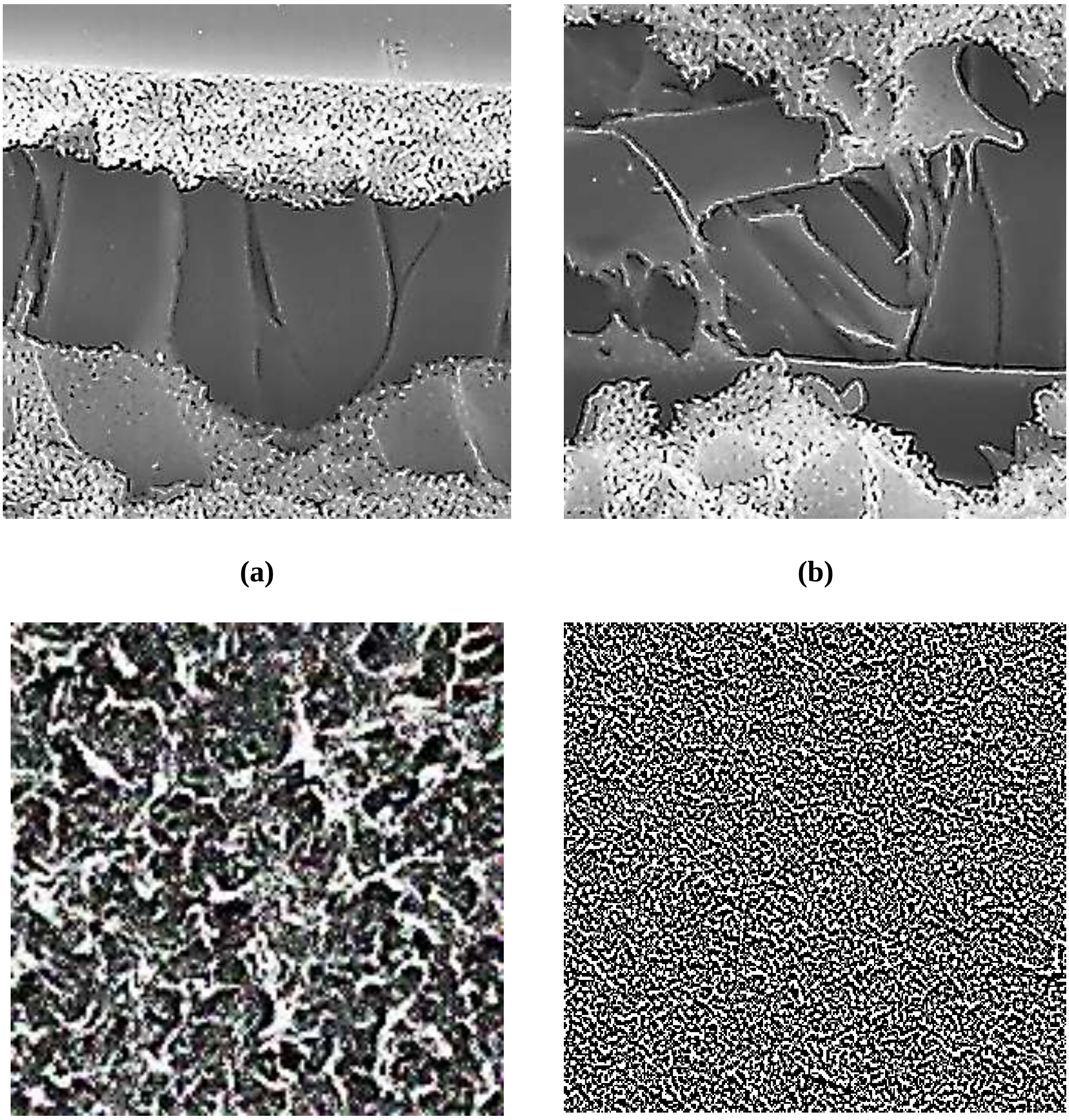

(a) (b)

(c) (d)

Fig. 2. SEM images of **(a)** NF270, **(b)** NF90, **(c)** BW30 and **(d)** SW30 membranes, respectively, in leather industry wastewater. (SEM images scale: 200 nm).

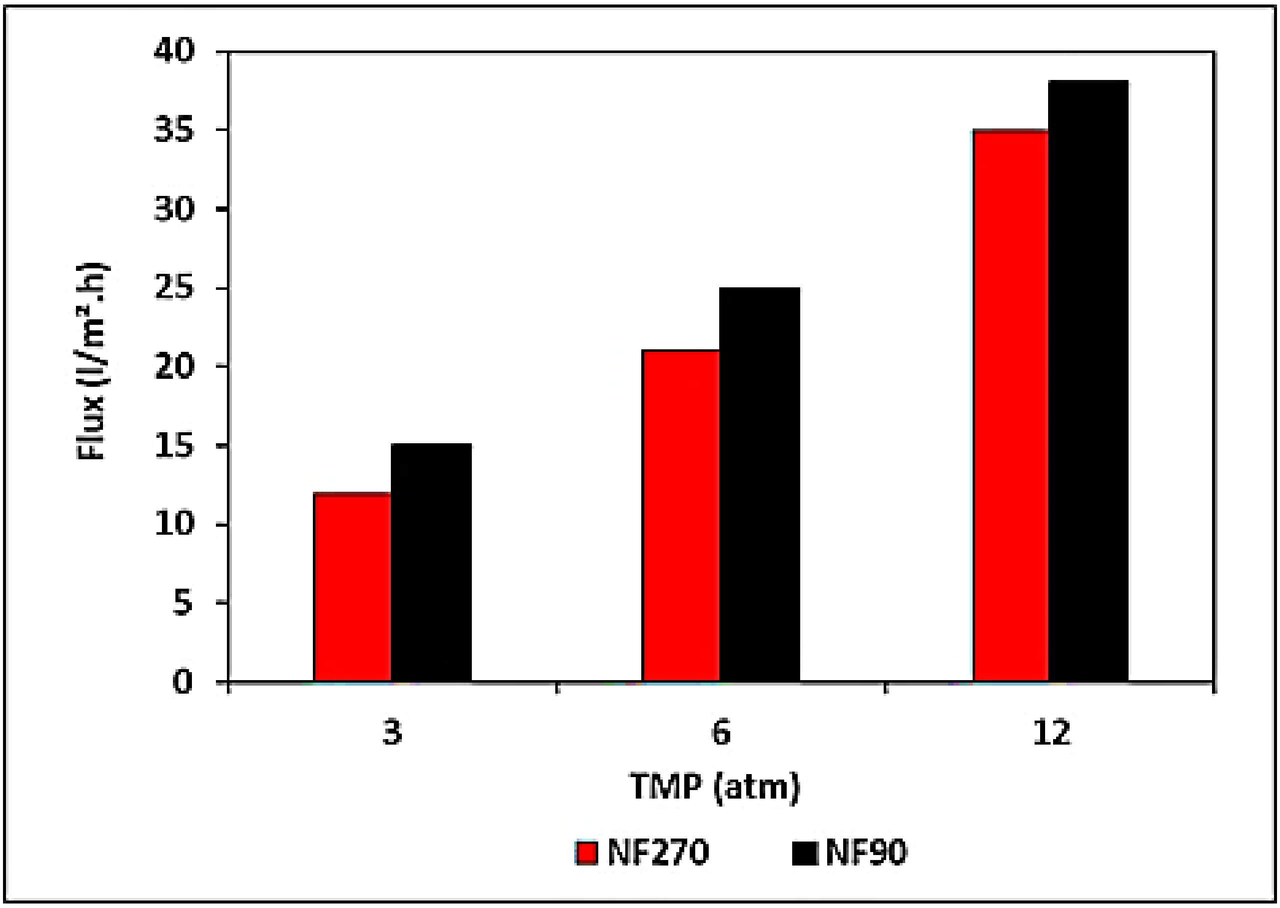

Fig. 3. Effect of TMP on NF (NF270 and NF90) flux at 30°C.

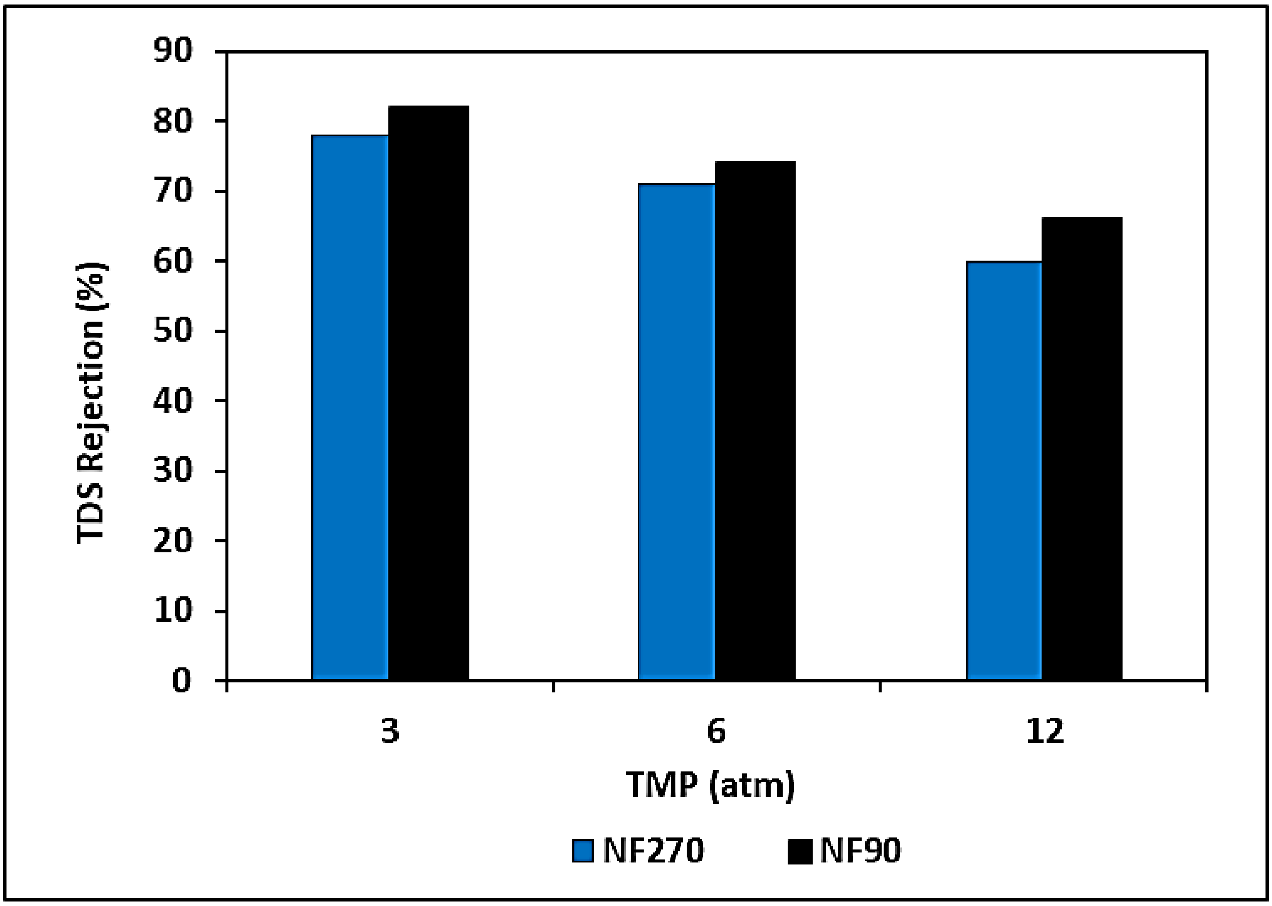

Fig. 4. The TDS rejection yields versus TMP on NF (NF270 and NF90) at 30^{o}C.

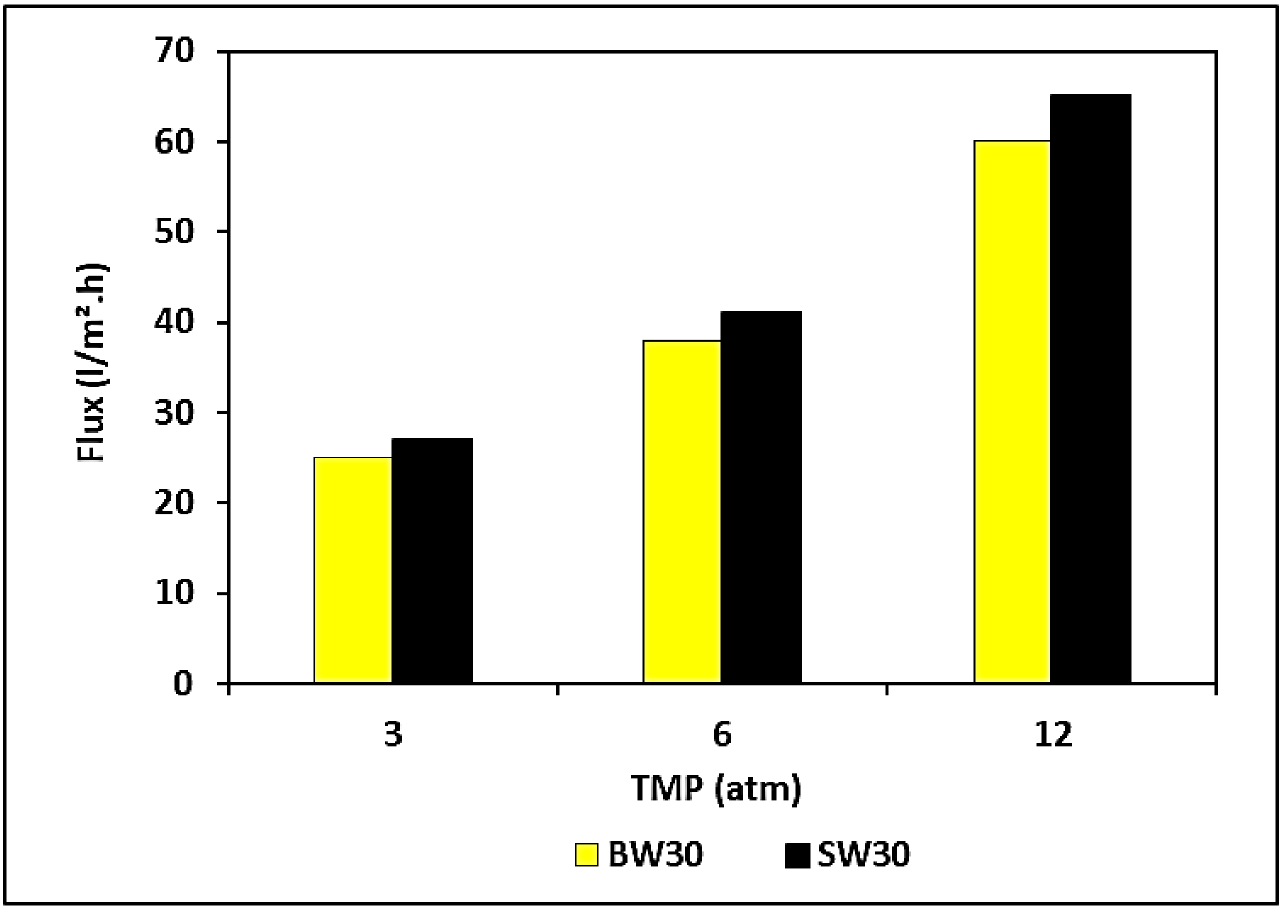

Fig. 5. Effect of TMP on RO (BW30 and SW30) flux at 30°C.

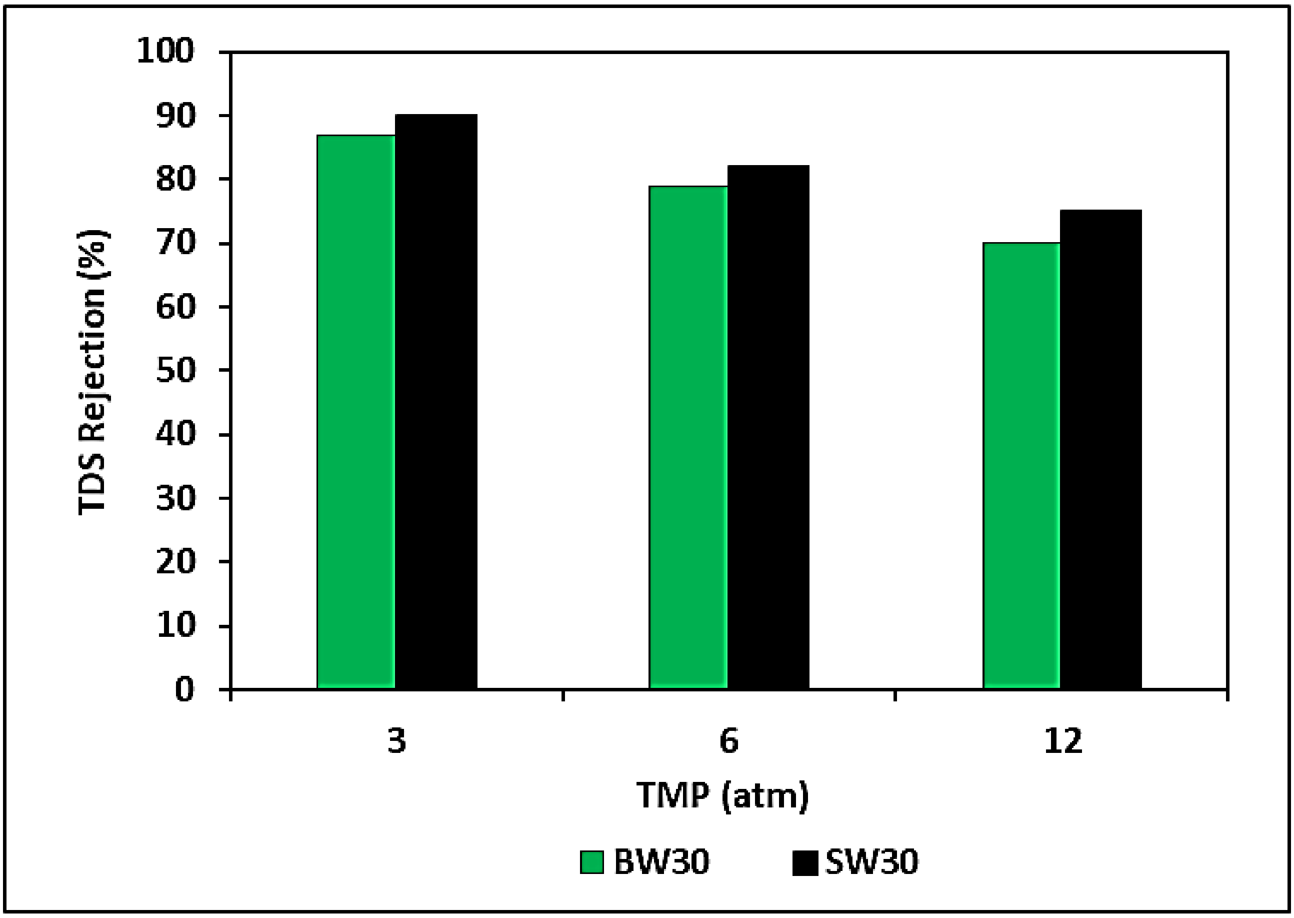

Fig. 6. The TDS rejection yields versus TMP on RO (BW30 and SW30) at 30°C.

Table 4. The removal efficiencies after NF and RO membrane processes in leather industry wastewater.

Parameters	NF Membranes		RO Membranes	
	NF270	NF90	BW30	SW30
COD_{total}	75	78	90	99
COD_{dis}	71	75	86	98
DOC	59	64	73	98
Inert COD	40	71	79	98
Na^{+}	20	80	85	99
K^{+}	18	72	82	99
Mg^{2+}	63	95	97	99
Ca^{2+}	58	97	98	99

Table 5. The recoveries of Cr, DCM and TCE in leather industry wastewater with NF and RO membranes.

Parameters	NF Membranes		RO Membranes	
	NF270	NF90	BW30	SW30
Cr Recovery (%)	77	82	95	99
Cr Recovery (mg/l)	435	643	870	945
DCM Recovery (%)	72	83	91	99
DCM Recovery (mg/l)	300	340	400	460
TCE Recovery (%)	66	80	88	99
TCE Recovery (mg/l)	200	232	300	360

Table 6. The comparison between experimental yields and ANN yields at 30ºC for Pearson correlation coefficient (r^2) and mean standard error (MSE)

Parameters	NF Membranes						RO Membranes					
	NF270	ANN		NF90	ANN		BW30	ANN		SW30	ANN	
	Removal (%)	Pearson correlation coefficient (r^2)	Mean standard error (MSE)	Removal (%)	Pearson correlation coefficient (r^2)	Mean standard error (MSE)	Removal (%)	Pearson correlation coefficient (r^2)	Mean standard error (MSE)	Removal (%)	Pearson correlation coefficient (r^2)	Mean standard error (MSE)
COD_{total}	75	0.96	0.0002	78	0.97	0.0001	90	0.99	0.0001	99	0.99	0.0001
COD_{dis}	71	0.96	0.0002	75	0.97	0.0002	86	0.98	0.0001	99	0.99	0.0001
DOC	59	0.98	0.0001	64	0.97	0.0002	73	0.98	0.0002	99	0.99	0.0001
Inert COD	40	0.97	0.0001	71	0.98	0.0002	79	0.98	0.0002	98	0.99	0.0001
Na^+	20	0.96	0.0003	80	0.98	0.0001	85	0.98	0.0002	99	0.99	0.0001
K^+	18	0.96	0.0003	72	0.96	0.0020	82	0.96	0.0003	99	0.97	0.0001
Mg^{2+}	63	0.97	0.0002	95	0.98	0.0001	97	0.99	0.0002	99	0.99	0.0001
Ca^{2+}	58	0.98	0.0001	97	0.99	0.0001	98	0.98	0.0002	99	0.99	0.0001
Recoveries	NF270	ANN		NF90	ANN		BW30	ANN		SW30	ANN	
	Recovery (%)	Pearson correlation coefficient (r^2)	Mean standard error (MSE)	Recovery (%)	Pearson correlation coefficient (r^2)	Mean standard error (MSE)	Recovery (%)	Pearson correlation coefficient (r^2)	Mean standard error (MSE)	Recovery (%)	Pearson correlation coefficient (r^2)	Mean standard error (MSE)
Cr Recovery (%)	77	0.96	0.0003	89	0.97	0.0002	95	0.99	0.0001	99	0.99	0.0001
Cr Recovery (mg/l)	35	0.96	0.0003	40	0.96	0.0003	870	0.98	0.0001	945	0.99	0.0001
DCM Recovery (%)	72	0.97	0.0002	83	0.98	0.0002	91	0.98	0.0002	99	0.99	0.0001
DCM Recovery (mg/l)	43	0.98	0.0001	50	0.96	0.0003	400	0.98	0.0002	460	0.99	0.0001
TCE Recovery (%)	66	0.95	0.0004	80	0.98	0.0002	88	0.98	0.0002	99	0.99	0.0001
TCE Recovery (mg/l)	17	0.95	0.0004	21	0.97	0.0002	300	0.99	0.0001	360	0.99	0.0001